Published in final edited form as:
*Spine J.* 2012 May ; 12(5): 425–432. doi:10.1016/j.spinee.2012.04.001.

# Height and Torsional Stiffness are Most Sensitive to Annular Injury in Large Animal Intervertebral Discs

**Arthur J Michalek**[1] and **James C Iatridis**[2]

[1]College of Engineering and Mathematical Sciences, The University of Vermont, Burlington, VT, USA

[2]Leni and Peter W. May Department of Orthopaedics, Mount Sinai School of Medicine, New York, NY, USA

### Keywords

intervertebral disc; injury; biomechanics; animal model

## Introduction

Acute injury to the annulus fibrosus (AF) has been implicated in the initiation of intervertebral disc (IVD) degeneration. Both biological [1-3] and mechanical [4-8] consequences result from these injuries. Despite the extensive use of animal models in the study of mechanical changes following acute AF injury, as recently reviewed [9], a complete picture of how injury affects a large animal IVD under multiple modes of loading is lacking. An additional aspect missing from the literature is the measurement of force coupling behavior. For example, axial compression or torsion of a symmetric disc should result in no bending moments, yet an injury to one side of the disc is expected to affect stiffness asymmetrically inducing a bending moment under compression, which may in turn compromise the stability of the spinal column. The extent to which this effect occurs as a result of acute AF injury is currently unknown.

In addition to studying the consequences of acute injury, large animal models are useful for investigating disc repair techniques both in vitro and in vivo [10-13]. A key challenge in developing strategies to replace the nucleus pulposus (NP) of a degenerated or herniated disc with either an artificial or tissue engineered construct is maintaining the integrity of the AF.

In addition to compromising fiber integrity it has been proposed that annular injury also results in an altered fluid flow behavior under load. This effect has thus far been inferred from experimental loading data either through comparison with permeability models [14, 15] or through comparison of loading modes expected to induce differing amounts of pressurization[16]. Direct pressurization experiments through a discomanometer showed decreased injection rupture pressure with increasing needle size, but did not address large annular tears [17]. In small animal models, the mechanical and biological effects of a



Corresponding Author: James C. Iatridis, PhD, Leni and Peter W. May Department of Orthopaedics, Mount Sinai School of Medicine, One Gustave L. Levy Place, Box 1188; New York, NY 10029, james.iatridis@mssm.edu.

puncture injury were highly dependent on whether or not the injury fully penetrated the AF [18]. It is currently unknown whether annular tears, in addition to compromising fiber integrity, directly result in altered fluid flow in the absence of loading.

This is a comprehensive study that aims to quantify the mechanical consequences of multiple injury types on multiple mechanical parameters using multiple degree of freedom testing in a single large animal model. We hypothesize that mechanical changes will be sensitive to size, location, and orientation of the injury. Furthermore, large annular injuries are expected to result in altered coupling between compressive, torsional, and bending mechanics, which are indicative of compromised spinal column stability. We further hypothesize that large annular injuries result in altered fluid flow behaviors under step pressurization by way of both altered radial bulging and increased effective permeability. These hypotheses were tested by subjecting bovine caudal IVDs to a sequential injury protocol and measuring mechanical parameters in four degrees of freedom: axial compression, axial torsion, flexion-extension, and lateral bending, as well as NP fluid pressurization before and after injury.

## Methods

### Specimen Preparation

Specimens were obtained from levels c2-3 through c5-6 of tails from skeletally mature steers obtained from a local abattoir. Following the removal of all surrounding muscle and ligaments, each vertebrae was sawn through its mid plane yielding motion segments consisting of two hemi-vertebrae and a disc. Wood screws were placed into the hemi-vertebrae, and they were then potted in PMMA (Schein Dental). The specimens were then wrapped in saline soaked tissue paper, placed in plastic bags, and frozen at -20°C until testing.

### Testing - Mechanical

Mechanical testing of the bovine motion segments was carried out using a custom built hexapod testing robot [19]. The protocol began with a 30 minute preload with 80N of compressive force, which corresponded to 0.2±0.05MPa stress, previously reported to be in the range of resting compressive stress for animal tails [20]. The following displacement/rotation controlled test was then performed four times; axial compression at ±0.3mm, axial torsion at ±2°, flexion-extension at ±2°, and lateral bending at ±2°. All tests were sinusoidal with ten cycles at 0.1Hz, the tenth cycle of which was used for analysis. The specimens were returned to 80N of axial compression between each step. Each motion segment was randomly assigned to one of three groups. Group A (n=4) served as a control, with no interventions during testing. Groups B and C (n=5) were subjected to injury, starting with a 21G needle puncture to a depth of 10mm on the anterior side of the disc at mid height between the first and second repetitions of the test protocol. Group B was subjected to a vertical incision to the lateral side of the disc between the second and third tests and a horizontal incision to the anterior side at the distal vertebral rim between the third and fourth tests. Group C was subjected to a horizontal incision between the second and third tests followed by a vertical incision between the third and fourth tests. All incisions were performed using a #22 scalpel blade inserted to a depth of 10mm. The positions of these injuries relative to the applied forces, displacements, and rotations are detailed in Figure 1. Throughout the protocol, the discs remained loosely wrapped with saline soaked tissue paper in order to maintain hydration.

### Testing - Fluid

Fluid pressurization behavior was measured using a custom built, trans-endplate saline pressurization instrument, similar to one previously used to measure high pressure disc failure mechanisms [21]. The instrument (Figure 2) consisted of a canulated stainless steel lag screw, which was inserted into a predrilled hole through the PMMA potting material and proximal vertebrae. The screw was attached via a compression fitting to pipes branching off to a pressure transducer (Omega PX302-1KGV) and syringe. Once the system was filled with saline, the syringe was compressed by hand until the pressure reached approximately 0.5MPa, as indicated by a calibrated panel meter. A check valve prevented saline from flowing back into the syringe. The fluid pressure in the disc was then allowed to equilibrate for thirty minutes. This procedure was repeated four times. The first trial served as a pre-conditioning and hydration step, and the second step was considered a baseline test. For injured specimens (n=5), the third and fourth steps followed puncture with a 21G needle and an axial incision with a #22 scalpel blade. Control specimens (n=5) were compressed four times in series with no intervention. As with the mechanical tests, hydration was maintained by keeping the discs wrapped in saline soaked tissue paper throughout the duration of the test. In order to keep fluid flow effects separated from solid matrix creep effects, the motion segments were constrained axially during testing.

### Data Analysis

Force and displacement data from the mechanical tests were analyzed using a custom written Matlab code. In order to reduce noise, compressive force was fit by $F(t) = F_0 \sin(\omega t + \delta)^{\beta}$. Torques resulting from torsional and bending rotations were represented by $T(t) = T_0 \sin(\omega t + \delta)$. Representative force-displacement and torque-rotation traces for an injured specimen are shown in Figure 3. Force and torque amplitudes were divided by displacement and rotation amplitudes to yield reduced stiffness matrices with axial compressive, axial torsion, flexion-extension, and lateral bending terms on the diagonals, as well as off-diagonal coupling terms. An estimate of motion segment viscosity was produced by calculating the difference in phase angle, $\delta$, between each applied displacement or rotation and the resultant forces and torques. In order to account for interspecimen variability, all stiffness and phase angle values were normalized to those obtained during the baseline mechanical test for each specimen.

In addition to stiffness and phase angle calculations, change in disc height was recorded continuously throughout the test. An additional Matlab code was used to manually digitize disc height before and after scalpel injury (Figure 4).

Pressurization data were analyzed using an additional Matlab code, which fit the following four parameter model to the recorded time dependent fluid pressure, $P(t)$.

$$P(t)=P_0 - S_1\left(1 - e^{-t/T_1}\right) - S_2\left(1 - e^{-t/T_2}\right)$$

In this function, $P_0$ is peak ramp pressure, $S_1$ and $S_2$ are short and long time scale pressure drops, and $T_1$ and $T_2$ are short and long time constants. Curve fit parameters from the post-puncture and post-incision ramps were normalized those from the baseline ramp in order to account for interspecimen variability.

### Statistics

Normalized mechanical test parameters (stiffness and phase angle) were analyzed using a two way anova to measure the effects of test type (control, vertical incision first, or rim incision first) and test step. Un-paired t-tests, with Welch's correction for unequal variance, were used as a post-hoc test to compare stiffness, phase angle, and height loss between injured and control groups. Two way anova was also used to analyze the effects of test type (control or injured) and test step on normalized curve fit parameters from the pressurization test. Un-paired t-tests, with Welch's correction for unequal variance, were used as a post-hoc test to compare control and injured groups at each step.

## Results

### Mechanical Test

Absolute stiffness and phase values pooled from the baseline tests of all specimens (n=14) are shown in Table 1. The two way anova showed no significant effects of test type, test step, or interaction on any stiffness or phase angle parameter ($p>0.1$). Differences between injured and control groups were insignificant ($p>0.1$) for all parameters except stiffness and phase under axial torsion, with stiffness being reduced incrementally by each incision and phase angle being reduced following both incisions (Figure 5). In the intact state, there was a marginally significant ($p=0.052$) difference in bending stiffnesses, being an average of 1.6 times higher in lateral bending than flexion-extension.

All injuries resulted in an instantaneous increase in height upon instrument (needle or scalpel) insertion followed by an instantaneous loss upon removal (Figure 6a). The instantaneous height loss was significantly higher for both vertical and rim incisions than for needle puncture, with vertical incisions resulting in slightly more height loss than rim incisions. Total height loss over the course of the experiment for specimens in both injury groups was significantly greater than control beginning with the first scalpel incision (Figure 6b).

### Pressurization Test

The fluid de-pressurization test showed large interspecimen variability, with $S_1$, $T_1$, $S_2$, and $T_2$, having mean baseline values ±SD of 0.31±0.23MPa, 40±75s, 0.11±0.073MPa, and 2900±3400s, respectively. The baseline values were thus used to normalize subsequent measurements for comparison. Average normalized parameter values from Equation 1 are shown in Table 2. While the anova indicated a significant effect of test type (control or injured) on long time constant ($T_2$), the t-tests did not show significance at any step. There was no apparent difference in pressure drop terms, $S_1$ and $S_2$, between injured and control specimens. Needle puncture had no effect on either time constant, while scalpel incision increased the short time constant, $T_1$, and decreased the long time constant, $T_2$, relative to control. Normalized curve fits, showing the effects of these changes in time constants are given in Figure 7.

## Discussion

This study quantified the effects of acute annular injury in multiple degrees of freedom of bovine caudal IVDs in order to provide a comprehensive evaluation of the effects of injury on IVDs. This study also provided the most comprehensive picture to date of biomechanical behaviors of intact bovine caudal motion segment, which are an animal model of increasing relevance due to their availability, large size, fibrous NP, and utility in many organ culture models. The key findings of this study were that disc height and torsional stiffness were the most sensitive properties to annular injury. Instantaneous height loss is likely related to the

release of residual circumferential strain in the AF [22]. Annular incision also resulted in slower short time scale and faster long time scale draining following NP fluid pressurization. Mechanical testing showed that vertically oriented incisions at the disc mid plane decreased torsional stiffness by a larger amount than horizontally oriented incisions at the vertebral rim, which can be explained by the annular fiber helical angle being less than 90° from circumferential causing a vertical incision to sever a larger percentage of the total number of annular fibers than a rim incision of the same size. This is consistent with previous findings at the tissue level showing a decrease in tensile stiffness proportional to the extent of fiber breakage [23].

These measurements provide important context for the development of IVD injury models and evaluation of repair techniques. A major barrier to the implementation of engineered tissue repair strategies, such as NP replacement, is the required incision of the AF and its subsequent repair. As expected from the strong relationship between torsional stiffness and intact AF fibers, our findings show that torsional loading under resting compression is most sensitive to AF integrity. Restoration of baseline motion segment torsional stiffness is thus likely to be the most sensitive benchmark for in vitro tests of AF repair methods. The results of this study also show that disc height loss occurs acutely, as well as progressively, following AF incision, suggesting that proper closure of incision sites may maintain disc height in both the short and long term.

While prior studies have found both increases and decreases in bending stiffness following injury [4, 5, 24, 25] these properties were the least sensitive to injury in the present study. Compressive stiffness has likewise been shown to be either insensitive to [7, 26, 27] or diminished by [16, 28, 29] annular injury. This apparent contradiction is most likely the result of the nonlinearity of the disc tissue’s compressive stiffness and differences in biomechanical testing protocols. Since the injured discs lost more height than control under physiological resting compressive stress, the un-injured portions of the disc became stiffer in compression countering any potential loss of overall compressive stiffness due to loss of pressurization or structural disruption. This is consistent with previous findings of increased motion segment stiffness with increased axial compressive strain [30]. The lack of an observed increase in bending moments under axial compression in injured disc in the current study further suggests that the fibrous NP of large discs supports a significant compressive load. This supports previous findings that catastrophic AF failure (prolapse) requires both fissuring of the AF and fragmentation of the NP [31]. Taken together, it seems clear that retaining IVD height during stiffness testing will result in loss of IVD axial and/or bending stiffness behaviors, yet with a controlled axial force during biomechanical testing (or follower load), a loss of IVD height and torsional stiffness become the more sensitive biomechanical parameters,

It is interesting to note that the mean stiffness values for lateral bending are more than one and a half times higher than those for flexion-extension (Table 1). This is contrary to the common assumption that due to their nearly cylindrical shape, bovine IVDs are axisymmetric. The discs used in this study had an average anterior-posterior:lateral aspect ratio of 0.957±0.117, which is comparable to the value of 0.962 reported previously [32]. There does, however, appear to be distinct differences in AF lamellar thickness between the anterior, posterior, and lateral sides of the disc which are likely to contribute to these functional differences (Figure 8). While caudal IVDs are substantially more axisymmetric than IVD from other levels, findings indicate that maintaining orientation is important during motion segment testing and may also be useful for minimizing variance while sampling tissue for other measurements.

The NP pressurization test was not sensitive to small injuries, yet it suggested that large disruptions do alter fluid flow pathways. The increase in short time constant and decrease in long time constant is consistent with prior findings [33], which suggest that short time scale behavior is governed mostly by annulus bulging, with fluid flow influencing longer time scales. This paints a picture of an injured disc which bulges more readily under compression (due to diminished annular integrity), then drains more quickly (as a result of reduced effective permeability). The lack of difference in pressure drop parameters between control and injured discs is consistent with the hypothesis that resting pressure in the NP results only from proteoglycan density [34]. Hydrostatic pressurization and fluid transport patterns were influenced by AF injury due to altered boundary conditions in rat caudal IVDs following needle puncture [15, 16]. The lack of clearly observable alterations in pressurization following injury in the current study suggests that fluid transport patterns in the more fibrous bovine IVD are governed more strongly by tissue material behaviors.

The use of bovine rather than human IVDs was chosen in this study for several reasons. Primarily, the IVDs used in this study came from a population which was relatively homogenous in both genetic makeup and age. This reduced the chances of the effects of artificially induced injuries being confounded by existing fissures or other degeneration patterns as would be found in human IVDs. Additionally, animal models are an important tool in developing disc repair techniques and thorough characterization of their response to injury is essential for success, and bovine caudal IVDs are of growing relevance in the spine field. It should, however, be noted that mature bovine discs are most structurally similar to human discs with a Thompson grade of 2 [35], and that how structural contributions of the NP and AF are changed by injury in more degenerated discs remains an important area of future study.

## Conclusions

Penetrating annular injuries lead to changes in intervertebral disc mechanics and present specific challenges to repair. While small injuries have been shown to affect tissue integrity at the small scale both biologically [36] and mechanically [37], whole motion segment tests were not sensitive enough to detect these acute defects except for small alterations in IVD height. Larger annular defects, arising from naturally occurring fissures or incisions, predominantly affect disc height under resting compressive load, torsional stiffness, and relaxation following NP pressurization. The complex interplay between disc height loss, tissue compressive nonlinearity, and motion segment stiffness in modes of loading which induce significant compression (axial compression, bending, and flexion-extension) needs to be carefully considered in developing test protocols to measure both the effects of annular injury and the efficacy of repair methods.

## Acknowledgments

This work was made possible by financial support from the National Institutes of Health (R01AR051146, 1R01 AR057397 and T32HL007944), by the AO Research Fund of the AO Foundation (Project no. F-09-10I), and assistance from Dr. Ian Stokes and Mr. Mack Gardner-Morse with usage of the hexapod testing apparatus.

## References

1. Han B, Zhu K, Li FC, Xiao YX, Feng J, Shi ZL, Lin M, Wang J, Chen QX. A simple disc degeneration model induced by percutaneous needle puncture in the rat tail. Spine. 2008; 33(18): 1925–34. [PubMed: 18708924]
2. Sobajima S, Kompel JF, Kim JS, Wallach CJ, Robertson DD, Vogt MT, Kang JD, Gilbertson LG. A slowly progressive and reproducible animal model of intervertebral disc degeneration characterized by MRI, X-ray, and histology. Spine. 2005; 30(1):15–24. [PubMed: 15626975]

3. Rousseau MA, Ulrich JA, Bass EC, Rodriguez AG, Liu JJ, Lotz JC. Stab incision for inducing intervertebral disc degeneration in the rat. Spine. 2007; 32(1):17–24. [PubMed: 17202887]
4. Thompson RE, Pearcy MJ, Barker TM. The mechanical effects of intervertebral disc lesions. Clin Biomech (Bristol, Avon). 2004; 19(5):448–55.
5. Thompson RE, Pearcy MJ, Downing KJ, Manthey BA, Parkinson IH, Fazzalari NL. Disc lesions and the mechanics of the intervertebral joint complex. Spine. 2000; 25(23):3026–35. [PubMed: 11145814]
6. Fazzalari NL, Costi JJ, Hearn TC, Fraser RD, Vernon-Roberts B, Hutchinson J, Manthey BA, Parkinson IH, Sinclair C. Mechanical and pathologic consequences of induced concentric anular tears in an ovine model. Spine. 2001; 26(23):2575–81. [PubMed: 11725238]
7. Kaigle A, Ekstrom L, Holm S, Rostedt M, Hansson T. In vivo dynamic stiffness of the porcine lumbar spine exposed to cyclic loading: influence of load and degeneration. J Spinal Disord. 1998; 11(1):65–70. [PubMed: 9493772]
8. Keller TS, Holm SH, Hansson TH, Spengler DM. 1990 Volvo Award in experimental studies. The dependence of intervertebral disc mechanical properties on physiologic conditions. Spine. 1990; 15(8):751–61. [PubMed: 2237625]
9. Iatridis JC, Michalek AJ, Purmessur D, Korecki CL. Localized Intervertebral Disc Injury Leads to Organ Level Changes in Structure, Cellularity, and Biosynthesis. Cellular and Molecular Bioengineering. 2009; 2(3):437–447. [PubMed: 21179399]
10. Heuer F, Ulrich S, Claes L, Wilke HJ. Biomechanical evaluation of conventional anulus fibrosus closure methods required for nucleus replacement. Laboratory investigation. J Neurosurg Spine. 2008; 9(3):307–13. [PubMed: 18928230]
11. Bron JL, Helder MN, Meisel HJ, Van Royen BJ, Smit TH. Repair, regenerative and supportive therapies of the annulus fibrosus: achievements and challenges. Eur Spine J. 2009; 18(3):301–13. [PubMed: 19104850]
12. Alini M, Roughley PJ, Antoniou J, Stoll T, Aebi M. A biological approach to treating disc degeneration: not for today, but maybe for tomorrow. Eur Spine J. 2002; 11(Suppl 2):S215–20. [PubMed: 12384747]
13. Wilke HJ, Heuer F, Neidlinger-Wilke C, Claes L. Is a collagen scaffold for a tissue engineered nucleus replacement capable of restoring disc height and stability in an animal model? Eur Spine J. 2006; 15(Suppl 3):S433–8. [PubMed: 16868784]
14. Hsieh AH, Wagner DR, Cheng LY, Lotz JC. Dependence of mechanical behavior of the murine tail disc on regional material properties: a parametric finite element study. J Biomech Eng. 2005; 127(7):1158–67. [PubMed: 16502658]
15. Michalek AJ, Iatridis JC. Penetrating annulus fibrosus injuries affect dynamic compressive behaviors of the intervertebral disc via altered fluid flow: an analytical interpretation. J Biomech Eng. 2011; 133(8):084502. [PubMed: 21950904]
16. Michalek AJ, Funabashi KL, Iatridis JC. Needle puncture injury of the rat intervertebral disc affects torsional and compressive biomechanics differently. Eur Spine J. 2010; 19(12):2110–6. [PubMed: 20544231]
17. Wang JL, Tsai YC, Wang YH. The leakage pathway and effect of needle gauge on degree of disc injury post anular puncture: a comparative study using aged human and adolescent porcine discs. Spine. 2007; 32(17):1809–15. [PubMed: 17762287]
18. Aoki Y, Akeda K, An H, Muehleman C, Takahashi K, Moriya H, Masuda K. Nerve fiber ingrowth into scar tissue formed following nucleus pulposus extrusion in the rabbit anular-puncture disc degeneration model: effects of depth of puncture. Spine. 2006; 31(21):E774–80. [PubMed: 17023838]
19. Stokes IA, Gardner-Morse M, Churchill D, Laible JP. Measurement of a spinal motion segment stiffness matrix. J Biomech. 2002; 35(4):517–21. [PubMed: 11934421]
20. MacLean JJ, Lee CR, Alini M, Iatridis JC. The effects of short-term load duration on anabolic and catabolic gene expression in the rat tail intervertebral disc. J Orthop Res. 2005; 23(5):1120–7. [PubMed: 16140193]
21. Schechtman H, Robertson PA, Broom ND. Failure strength of the bovine caudal disc under internal hydrostatic pressure. J Biomech. 2006; 39(8):1401–9. [PubMed: 15964006]

22. Michalek AJ, Gardner-Morse MG, Iatridis JC. Large Residual Strains are Present in the Intervertebral Disc Annulus Fibrosus in the Unloaded State. Journal of Biomechanics. 2012 In Press.

23. Adams MA, Green TP. Tensile properties of the annulus fibrosus I. The contribution of fibre-matrix interactions to tensile stiffness and strength. European Spine Journal. 1993(2):203–208.

24. de Visser H, Rowe C, Pearcy M. A robotic testing facility for the measurement of the mechanics of spinal joints. Proc Inst Mech Eng [H]. 2007; 221(3):221–7.

25. Schmidt TA, An HS, Lim TH, Nowicki BH, Haughton VM. The stiffness of lumbar spinal motion segments with a high-intensity zone in the anulus fibrosus. Spine. 1998; 23(20):2167–73. [PubMed: 9802156]

26. Boxberger JI, Sen S, Yerramalli CS, Elliott DM. Nucleus pulposus glycosaminoglycan content is correlated with axial mechanics in rat lumbar motion segments. J Orthop Res. 2006; 24(9):1906–15. [PubMed: 16865712]

27. Elliott DM, Yerramalli CS, Beckstein JC, Boxberger JI, Johannessen W, Vresilovic EJ. The effect of relative needle diameter in puncture and sham injection animal models of degeneration. Spine. 2008; 33(6):588–96. [PubMed: 18344851]

28. Hsieh AH, Hwang D, Ryan DA, Freeman AK, Kim H. Degenerative anular changes induced by puncture are associated with insufficiency of disc biomechanical function. Spine. 2009; 34(10): 998–1005. [PubMed: 19404174]

29. Korecki CL, Tuan RS, Iatridis JC. Notochord Cell Conditioned Medium Stimulates Mesenchymal Stem Cell Differentiation Toward a Young Nucleus Pulposus Phenotype. Trans Orthop Res Soc. 2008:1404.

30. Gardner-Morse MG, Stokes IA, Churchill D, Badger G. Motion segment stiffness measured without physiological levels of axial compressive preload underestimates the in vivo values in all six degrees of freedom. Stud Health Technol Inform. 2002; 91:167–72. [PubMed: 15457717]

31. Brinckmann P, Porter RW. A laboratory model of lumbar disc protrusion. Fissure and fragment. Spine. 1994; 19(2):228–35. [PubMed: 7864915]

32. O'Connell GD, Vresilovic EJ, Elliott DM. Comparison of animals used in disc research to human lumbar disc geometry. Spine (Phila Pa 1976). 2007; 32(3):328–33. [PubMed: 17268264]

33. Masuoka K, Michalek AJ, MacLean JJ, Stokes IA, Iatridis JC. Different effects of static versus cyclic compressive loading on rat intervertebral disc height and water loss in vitro. Spine. 2007; 32(18):1974–9. [PubMed: 17700443]

34. Urban JP, McMullin JF. Swelling pressure of the inervertebral disc: influence of proteoglycan and collagen contents. Biorheology. 1985; 22(2):145–57. [PubMed: 3986322]

35. Demers CN, Antoniou J, Mwale F. Value and limitations of using the bovine tail as a model for the human lumbar spine. Spine. 2004; 29(24):2793–9. [PubMed: 15599281]

36. Korecki CL, Costi JJ, Iatridis JC. Needle puncture injury affects intervertebral disc mechanics and biology in an organ culture model. Spine. 2008; 33(3):235–41. [PubMed: 18303454]

37. Michalek AJ, Buckley MR, Bonassar LJ, Cohen I, Iatridis JC. The effects of needle puncture injury on microscale shear strain in the intervertebral disc annulus fibrosus. Spine J. 2010; 10(12):1098–105. [PubMed: 20971041]

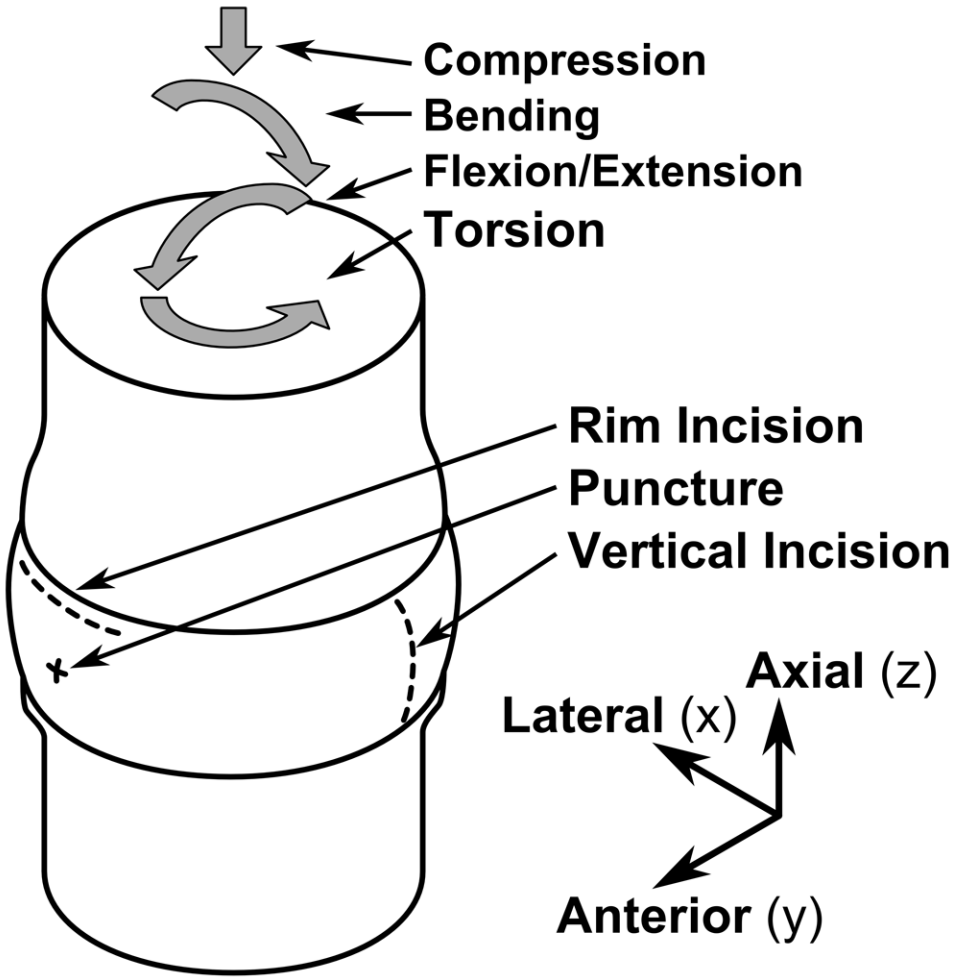


**Figure 1.**
Schematic of multiple degree of freedom motion segment test showing modes of loading and injury types. A 21G needle Puncture to a depth of 10mm was always performed first followed by Vertical Incision and Rim Incision with #22 scalpel blade inserted to 10 mm (Group B) or vice versa (Group C).

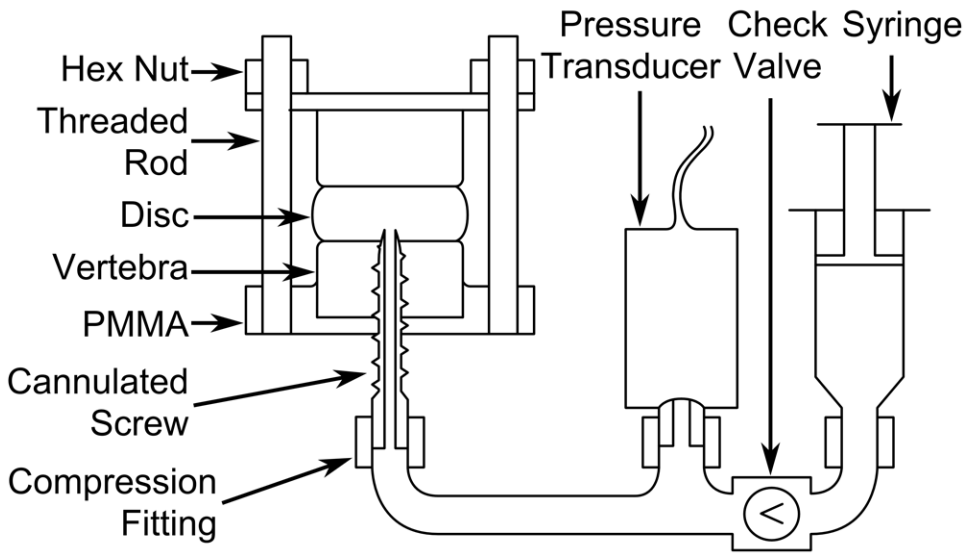


**Figure 2.**
Schematic of disc fluid pressurization apparatus consisting of a canulated stainless steel lag screw, which was inserted into a predrilled hole through the PMMA potting material and proximal vertebrae. The screw was attached to a pressure transducer and syringe. Once the system was filled with saline, the syringe was compressed to a pressure of 0.5MPa, and rate of pressure drop was recorded for 30 minutes before and after injury.

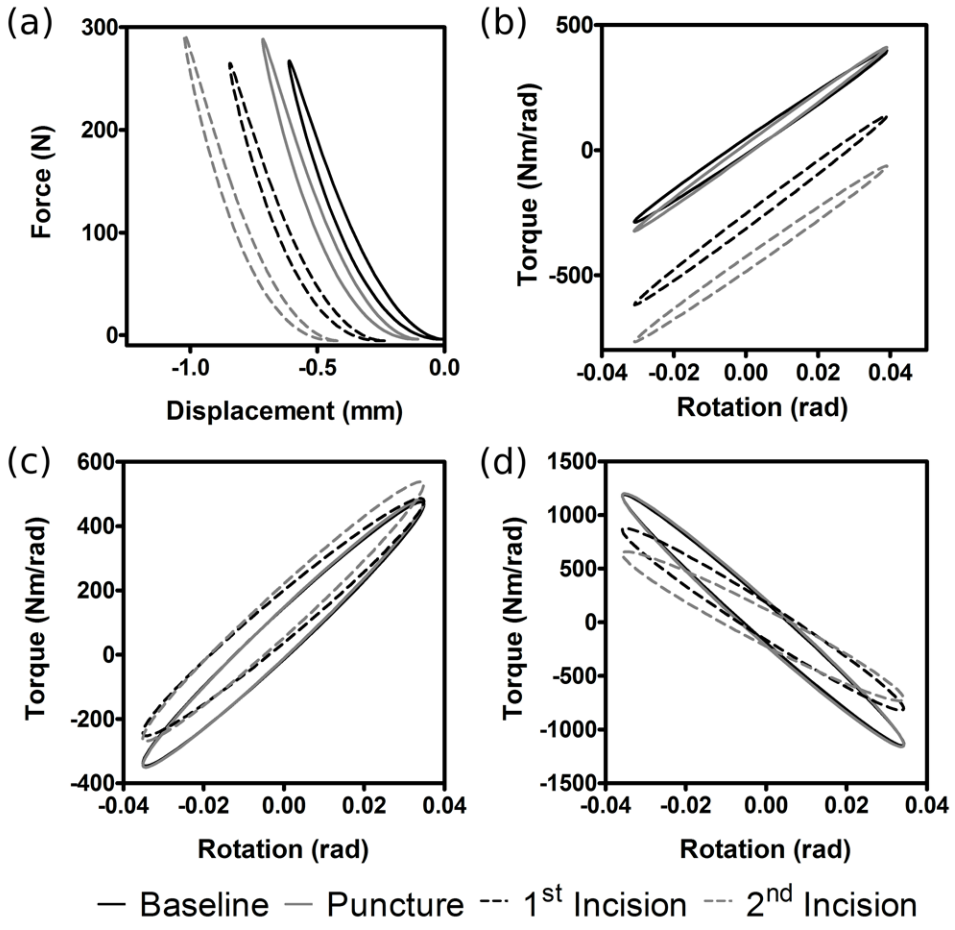


**Figure 3.**

Typical force-displacement and torque-rotation model fits for axial compression (a), flexion-extension (b), lateral bending (c), and axial torsion (d). Force and torque amplitudes were divided by displacement and rotation amplitudes to yield reduced stiffness matrices with axial compressive, axial torsion, flexion-extension, and lateral bending terms on the diagonals, as well as off-diagonal coupling terms. Data is shown for baseline test as well as following puncture and 2 additional scalpel incisions.

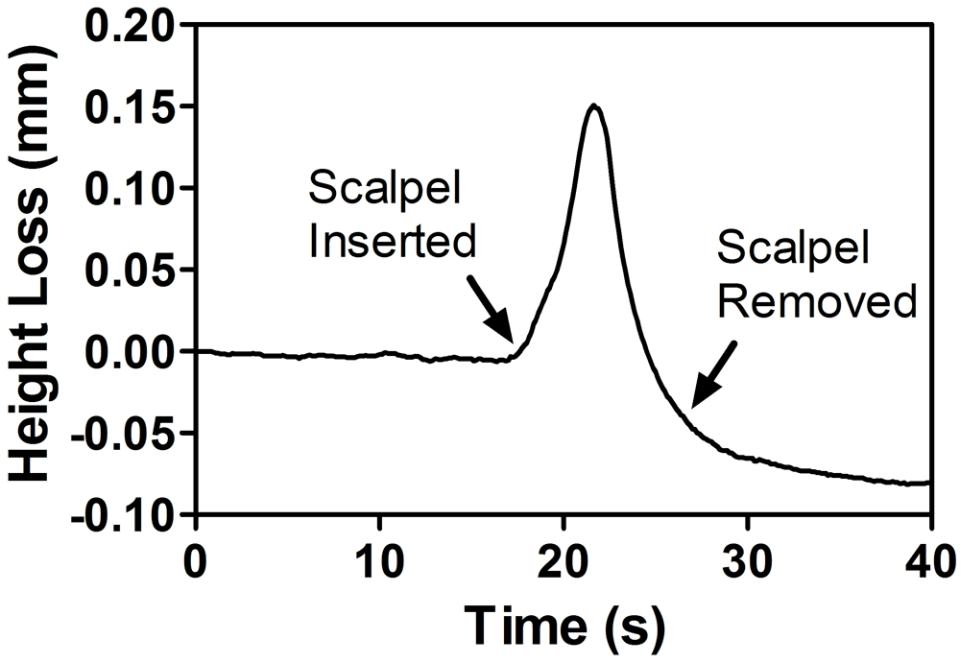


**Figure 4.**
Scalpel incision to the rim of the disc induced immediate, repeatable, but small magnitudes of height loss under static load. The instantaneous and cumulative height losses were measured throughout the experiment.

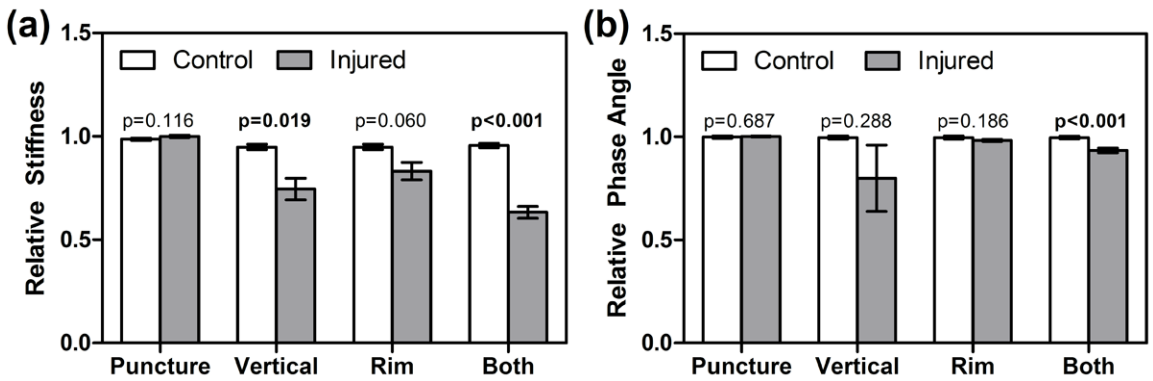


**Figure 5.**

Transient height loss, as shown in Figure 4, resulted in insignificant instantaneous height loss (a) for needle puncture, but significant instantaneous loss for vertical and rim incisions (p=0.364, <0.001, and 0.020 respectively). Cumulative height loss throughout the test protocol (b) was significant for all interventions except puncture.

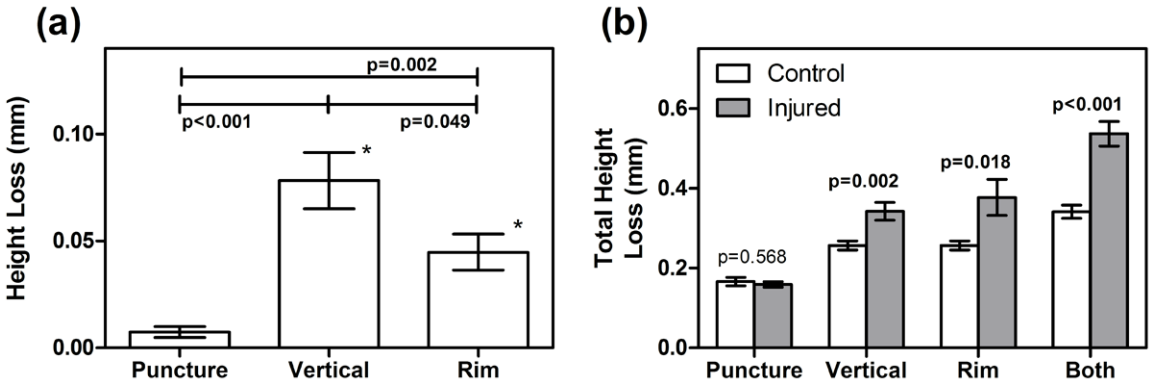


**Figure 6.**
Torsional stiffness (a) and phase angle (b) relative to baseline values.

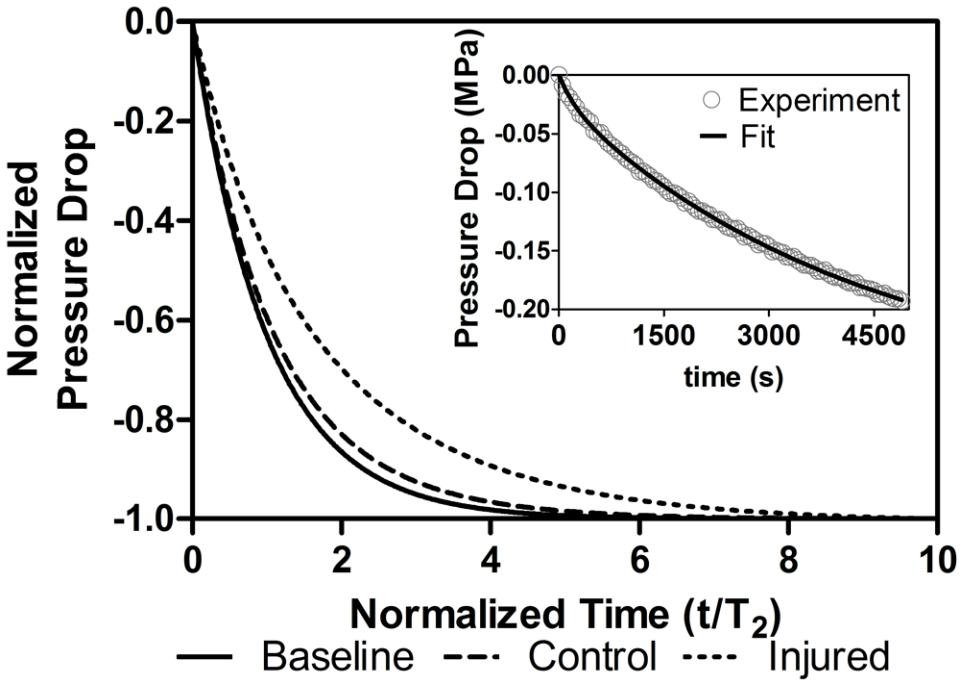


**Figure 7.**

Average disc de-pressurization curve fits illustrating the effect of time constant changes measured experimentally. Time and pressure drop are normalized to account for interspecimen variability. Insert shows typical curve fit to experimental pressure vs. time data. In this test, trans annular injury altered the transient pattern of pressure drop with an increase in short time constant (presumably because the IVD bulges more readily due to diminished annular integrity), and a decrease in long time constant (presumably due to an increase in fluid transport as a result of reduced effective permeability).

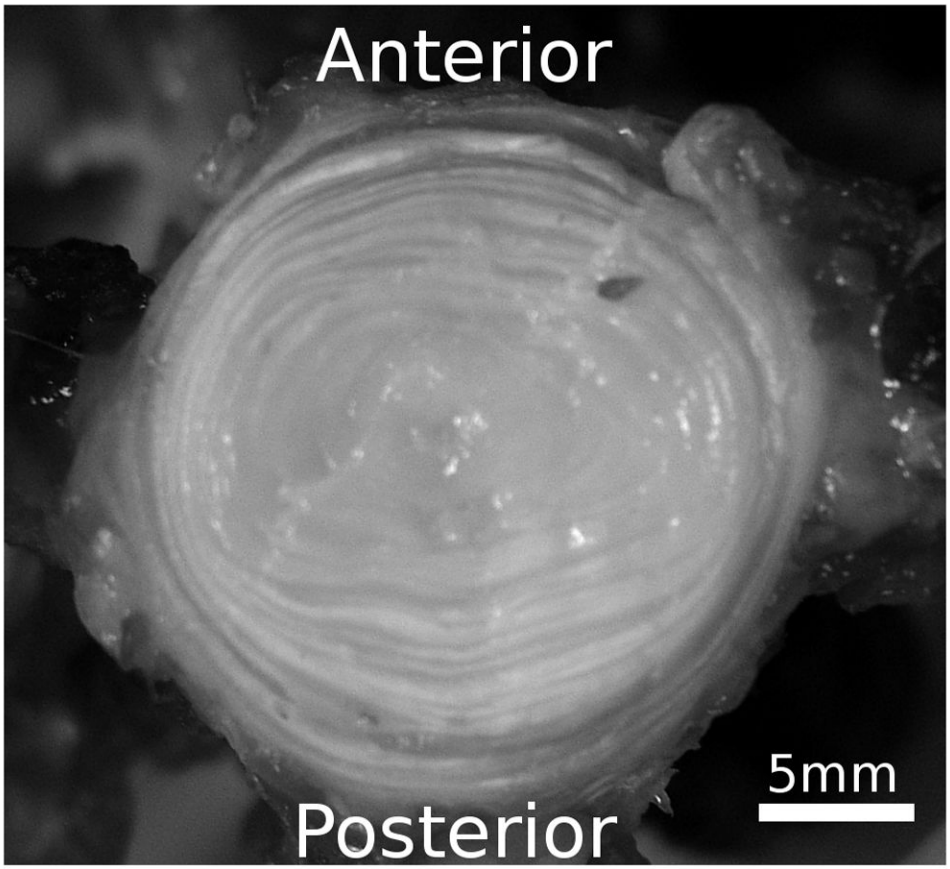


**Figure 8.**
Cross section of a bovine caudal IVD, showing distinct difference in lamellar thickness with anatomical location.

## Table 1

Multiple degree of freedom stiffness values of intact motion segments ± SD.

| | **$F_z$** | **$T_x$** | **$T_y$** | **$T_z$** |
|---|---|---|---|---|
| $d_z$ | 704±101 (1) | 4924±7214 (2) | 2839±4999 (2) | 2128±5780 (2) |
| $r_x$ | 0.97±1.10 (3) | 521±431 (4) | 2.00±1.20 (4) | 6.68±4.05 (4) |
| $r_y$ | 0.93±0.74 (3) | 1.96±1.56 (4) | 855±523 (4) | 10.79±6.16 (4) |
| $r_z$ | 0.33±0.21 (3) | 2.14±2.03 (2) | 4.88±4.59 (4) | 2673±2285 (4) |
| b) Axial and rotational phase angle values of intact motion segments Phase angles ± SD are in radians. | | | | |
| | $F_z$ | $T_x$ | $T_y$ | $T_z$ |
| $d_z$ | 1.47±0.01 | 1.2±0.51 | 0.58±0.62 | 0.79±0.32 |
| $r_x$ | 0.96±0.39 | 0.45±0.44 | 0.81±0.43 | 0.80±0.49 |
| $r_y$ | 0.71±0.39 | 0.69±0.53 | 0.61±0.53 | 0.62±0.35 |
| $r_z$ | 0.70±0.45 | 0.86±0.48 | 0.80±0.44 | 1.34±0.04 |

Stiffness was calculated as the force or torque ($F_Z$, $T_X$, $T_Y$, and $T_Z$) resulting from applied displacements and rotations ($d_Z$, $r_X$, $r_Y$, and $r_Z$). Coordinates are as shown in Figure 1. Values are in (1) N/mm with nonlinear exponent of 1.8±0.34, (2) Nm/N, (3) kN/° (4) Nm/°.

**Table 2**

Mean pressurization curve fit parameters, normalized to baseline values, ± SD.

| | **Control** | | | | **Injured** | | | |
|---|---|---|---|---|---|---|---|---|
| | **$S_1$** | **$T_1$** | **$S_2$** | **$T_2$** | **$S_1$** | **$T_1$** | **$S_2$** | **$T_2$** |
| Puncture | 1.00±0.14 | 0.92±0.24 | 0.84±0.12 | 0.88±0.48 | 1.03±0.15 | 1.55±0.47 | 0.88±0.14 | 0.90±0.15 |
| Incision | 1.11±0.12 | 0.89±0.08 | 0.90±0.34 | 1.45±0.80 | 1.01±0.20 | 2.14±1.18 | 0.78±0.13 | 0.82±0.20 |